electronics

MDPI

Article

A New Optimization Algorithm Based on the Fungi Kingdom Expansion Behavior for Antenna Applications

Falih M. Alnahwi [1], Yasir I. A. Al-Yasir [2,3,*], Dunia Sattar [4], Ramzy S. Ali [1], Chan Hwang See [5] and Raed A. Abd-Alhameed [2]

1 Department of Electrical Engineering, College of Engineering, University of Basrah, Basrah 61001, Iraq; fma3nc@mail.missouri.edu (F.M.A.); ramzy.ali@uobasrah.edu.iq (R.S.A.)
2 Faculty of Engineering and Informatics, University of Bradford, Bradford BD7 1DP, UK; R.A.A.Abd@bradford.ac.uk
3 Skyrora Ltd., Glasgow G68 9LD, UK
4 Department of Computer Engineering, College of Engineering, University of Basrah, Basrah 61001, Iraq; Dunia.tahir@uobasrah.edu.iq
5 School of Engineering and the Built Environment, Edinburgh Napier University, Edinburgh EH10 5DT, UK; C.See@napier.ac.uk
* Correspondence: y.i.a.al-yasir@bradford.ac.uk; Tel.: +44-127-423-8047

Abstract: This paper presents a new optimization algorithm based on the behavior of the fungi kingdom expansion (FKE) to optimize the radiation pattern of the array antenna. The immobile mass expansion of the fungi is mimicked in this work as a chaotic behavior with a sinusoidal map function, while the mobile mass expansion is realized by a linear function. In addition, the random germination of the spores is utilized for randomly distributing the variables that are far away from the best solution. The proposed FKE algorithm is applied to optimize the radiation pattern of the antenna array, and then its performance is compared with that of some well-known algorithms. The MATLAB simulation results verify the superiority of the proposed algorithm in solving 20-element antenna array problems such as sidelobe reduction with sidelobe ratio (SLR = 25.6 dB), flat-top pattern with SLR = 23.5 dB, rectangular pattern with SLR = 19 dB, and anti-jamming systems. The algorithm also results in a 100% success rate for all of the mentioned antenna array problems.

Keywords: fungi kingdom; antenna array; array factor; immobile mass; mobile mass

Citation: Alnahwi, F.M.; Al-Yasir, Y.I.A.; Sattar, D.; Ali, R.S.; See, C.H.; Abd-Alhameed, R.A. A New Optimization Algorithm Based on the Fungi Kingdom Expansion Behavior for Antenna Applications. *Electronics* **2021**, *10*, 2057. https://doi.org/10.3390/electronics10172057

Academic Editor: Xiaojing Huang

Received: 3 August 2021
Accepted: 23 August 2021
Published: 26 August 2021

1. Introduction

In recent years, the increasing complexity and difficulty of real applications have led to more efficient metaheuristic algorithms. Most of these algorithms use random variables and can estimate the best solutions for different fields of optimization problems [1]. Metaheuristic algorithms outperform traditional algorithms due to their gradient-free techniques and avoidance of dropping in local optima [2]. During the solving process of any optimization problem, metaheuristic algorithms depend on two techniques namely intensification and diversification [3]. Intensification searches for the best solution within the local search space while diversification explores the search space globally to avoid dropping in local optima. The outstanding performance of an algorithm demands an appropriate balance between these two techniques. All collective solutions-based algorithms employ these features but with various operators and strategies [1]. Metaheuristic collective solutions-based algorithms can be grouped based on various inspiration fields into seven categories: biology, physics, chemistry, mathematics, social/human, music, and sport/games.

Biology-based algorithms are categorized into two dominant groups: evolutionary algorithms and bio-based/swarm intelligence techniques. Evolutionary algorithms are simulated Darwin's theory of evolution. A genetic algorithm (GA) was the first evolutionary algorithm proposed by John Holland [4]. On the other hand, the second group of

biology-based algorithms includes bio/swarm intelligence-based algorithms that can be sub-categorized into seven classes based on their behavior of

1. Wild animals like grey wolf optimizer [5], camel algorithm [6], and wild horse optimizer [7].
2. Aquatic animals such as whale optimization algorithm [1] and salp swarm search [8].
3. Insects like ant colony optimization [9,10] and moth search algorithm [11].
4. Birds such as particle swarm optimization (PSO) [12] which has widely been used for antenna applications in recent years [13,14], bat algorithm [15], and African vultures optimization algorithm [16].
5. Plant such as plants tree growth optimization algorithm [17] and smart flower optimization algorithm [3].
6. Viruses as virus colony search [18] and coronavirus herd immunity optimizer [19].
7. Human body parts such as heart optimization algorithm [20] and kidney algorithm [21].

The second group of metaheuristic algorithms is the physics-based algorithms which simulate the physics rules in nature like Archimedes optimization algorithm [22] and atomic orbital search [23]. The third group that relies on chemistry in their optimization procedure such as artificial chemical reaction optimization [24] and gases Brownian motion optimization [25]. Math-based algorithms are the fourth category of metaheuristic algorithms that mimic the mathematical rules. The most common math algorithms are the sine cosine algorithm [26] and the arithmetic optimization algorithm [2]. Social/human algorithms are the fifth type of metaheuristic algorithms which include the student psychology optimization algorithm [27] and harmony search [28] which is a music-based algorithm. The last category is sports and games algorithms like football optimization algorithm [29] and billiards optimization algorithm [30].

Basically, the majority of high-gain antennas suffer from undesired sidelobe levels, and hence several approaches have been proposed to manipulate these kind of issues such as using all-metal wideband metasurface [31] and using non-uniform metallic lattice [32]. Moreover, the side lobes of the antenna radiation pattern can also be improved by manipulating the primary antenna phase [33] and placing a 3D superstructure in the nearfield [34].

In this paper, the Fungi Kingdom Expansion (FKE) behavior is utilized for optimizing the radiation pattern of the antenna array. The immobile and mobile mass expansions are emulated by a chaotic sinusoidal map function and linear deterministic function, respectively. The parameters that are far away from the best solution are randomly spread out to explore other more suitable locations. The proposed FKE algorithm is simulated using MATLAB to solve some of the array antenna beamforming problems like sidelobe reduction with SLR = 25.6 dB, flat-top pattern with SLR = 23.5 dB, rectangular pattern with SLR = 19 dB, and anti-jamming systems. After comparing the performance of the proposed algorithm with some other prominent algorithms, the results show the FKE algorithm has an almost flawless optimization performance in solving the antenna array problems.

2. Fungi Kingdom Expansion Behavior

The filamentous fungi shown in Figure 1 have a special form called mycelium [35]. Before extending their biomass, the fungi spread filament structures called (hyphae whose singular is hyphen) which begin the growth of the fungi kingdom in a form starting with the germination of spores. The expansion of the fungal colony is based on the availability of warmth and moisture within the surrounding area. The fungi extend their hyphae chaotically in different directions but within a small area to check the directions at which the amount of the moisture and warmth are suitable [35]. Subsequently, the biomass flows through tubes inside the hyphae toward the terminals of the hyphae that are oriented toward suitable conditions [35]. In concise, the materials that contribute to the fungi expansion behavior can be categorized into two types:

(a) Immobile biomass expansion: which represents the materials that are used to build the hyphae and the tubes inside them.
(b) Mobile biomass expansion: this part represents the material flowing through the tubes of the hyphae to provide nutrition to the terminal of the hyphae.

Figure 1. Filamentous fungi.

Therefore, the aforementioned behavior can be translated into an optimization algorithm that searches for the best solution to a certain problem. It is worth mentioning that the behavior of the Fungi in [35] is mimicked as a routing algorithm. In this work, the fungi expansion behavior is exploited to form an optimization algorithm that searches for a certain optimum solution that is not related to the routing problems at all.

3. Implementation of the Fungi Kingdom Expansion (FKE) Algorithm

Consider that $\boldsymbol{x^i} = \begin{bmatrix} x_1^i & x_2^i & \dots & x_{Dim}^i \end{bmatrix}$ represents the position of the $\boldsymbol{i}$-th fungus where $i = [1, 2, \dots, Pop]$, and Pop represents the population size of the fungi kingdom. The initial population distribution can be determined by randomly ($Rand$) spreading spores within the maximum allowed distance (x_{max}) and the minimum allowed distance (x_{min}) as given below:

$$\boldsymbol{x^{iter}} = (x_{max} - x_{min})Rand + x_{min} \tag{1}$$

where ***iter*** represents the iteration number which is equal to zero at the initial step.

Based on what has been mentioned in the previous section, the authors noticed that the fungi kingdom is expanded in three different modes:

- ***Mode 1:*** *Chaotic Expansion Mode*

This mode represents the generation of the hyphae for the immobile biomass expansion which is equivalent to the local searching mechanism. Since the fungi spread their hyphae in different directions but within a pre-determined area, this behavior is likely to be chaotic rather than random. Let the parameter (***hyp***) denote the hyphen number, then the proposed Equation that describes the immobile mass expansion is given as:

$$\boldsymbol{x^{i,hyp}} = \boldsymbol{x^i} + IEF \times \boldsymbol{F^{i,hyp}} \tag{2}$$

where IEF represents the immobile expansion factor and $\boldsymbol{F}$ represents the chaotic function which is selected to be the sine map function in this work:

$$\boldsymbol{F^{i,hyp}} = sin\left(\pi\, \boldsymbol{F^{i,hyp-1}}\right) \tag{3}$$

It is worth mentioning that the value of the IEF should not be too small because that results in too short hyphae, and the optimization process will take a very large number of iterations. In contrast, the value of IEF should not be too large in order not to lose the local searching property of this mode of expansion.

After evaluating the positions of the terminals of the hyphae, they should be applied to a certain fitness function to pick up the best local position among them ($\boldsymbol{x^{local\ best,iter}}$) for the present iteration (***iter***), and then the mobile mass expansion will be applied.

- ***Mode 2:*** *Deterministic Expansion Mode*

This mode is corresponding to the mobile biomass expansion in which the nutrition of the biomass is passed through the tube of the best hyphen. The Equation that is proposed to find the new location of each fungus in the population at the present iteration depending on the past iteration ($\boldsymbol{x^{iter-1}}$) and the present best local position ($\boldsymbol{x^{local\ best,iter}}$) is given by:

$$\boldsymbol{x^{iter}} = \boldsymbol{x^{iter-1}} + cond^{iter}\left(\boldsymbol{x^{local\ best,iter}} - \boldsymbol{x^{iter-1}}\right) \tag{4}$$

where *cond* represents the surrounding condition factor that is directly proportional to the moisture and the temperature. This factor can be evaluated from the following formula:

$$cond^{iter} = 1 - \frac{MT^{iter} - MT_{min}}{MT_{max} - MT_{min}} \tag{5}$$

where MT^{iter} denotes the Moisture-Temperature effect at the present iteration, MT_{max} and MT_{min} are the maximum and minimum Moisture-Temperature effect, respectively. MT^{iter} can be evaluated by randomly (*Rand*) selecting a value between MT_{max} and MT_{min} such that:

$$MT^{iter} = (MT_{max} - MT_{min})Rand + MT_{min} \tag{6}$$

After applying (4), (5), and (6) to the entire fungi population, the position of each of them is assessed by the fitness function to determine the global best position of the present iteration ($\boldsymbol{x^{global\ best,iter}}$).

- ***Mode 3:*** *Random Dispersion*

The random dispersion in the fungi kingdom happens when some of the population get far away from the nutrition sources. In this case, the fungi randomly germinate spores in random directions within the nutrition region bounded by the distance $[x_{min},\ x_{max}]$ exactly like that in Equation (1). The resulted population is also subjected to the fitness function to determine whether the global best location of the present iteration is more preferable to the previous best location or not. Thence, the new fungi population is generated, and the next iteration ($\boldsymbol{iter} + 1$) is started. This optimization sequence is repeated until the required condition is met, or the number of iterations is terminated. The pseudo-code of the proposed Fungi Kingdom Expansion (FKE) algorithm is given in Figure 2.

```
% FKE Pseudo-Code:
Set the moisture-temperature range and the location range.
Set the number of hyphae
Set the fungi kingdom size and the dimension.
Set the random dispersion number (DIS).
Initialize the location of each fungus from Eq. (1).
Subject the locations to a certain fitness function.
Determine the current best location.
Apply Eq. (3) for the entire population and entire iterations.
While (iter < iter_max)
    % The immobile mass expansion
 For i=1: fungi kingdom size
   For j=1: number of hyphae
        Apply Equation (2) with the aid of Eq. (3)
   End j
   Subject the hyphae to a fitness function then pick the best hyphen only.
     % The mobile mass expansion
        Compute (MT) from Eq. (6)
        Compute (cond) from Eq. (5)
        Apply Eq. (4)
 End i
   Subject the new locations to the fitness function
   If the new best location is better than the older one
        The new best is the global best
   End If
   Randomly spread the worst (DIS) locations
   Subject the new population to the fitness function to determine the global best.
End While
```

Figure 2. The pseudo-code of Fungi Kingdom Expansion (FKE) algorithm.

4. Engineering Applications: Antenna Array Beamforming

The proposed FKE algorithm is implemented using MATLAB to optimize the operation of the antenna array. Based on the no free lunch theorem [36], there is no optimization technique that can perfectly operate in all problems of optimization. However, the authors found that the FKE algorithm is quite flawless in solving the antenna array beamforming process. The structure of the M-element antenna array is illustrated in Figure 3a. The array factor of the entire array is given by:

$$AF = \boldsymbol{w}^{\boldsymbol{H}}\, \boldsymbol{a}(\Phi) \tag{7}$$

where $\boldsymbol{w}$ represents the weights vector that described the magnitude and the phase of the current that excites each element, the superscript $\boldsymbol{H}$ denotes the Hermitian transpose, and $\boldsymbol{a}(\Phi)$ represents the steering vector of the antenna at any azimuth angle (Φ):

$$\boldsymbol{a}(\Phi) = \begin{bmatrix} 1 \\ \exp[j\beta d_1 \cos(\Phi)] \\ \exp[j2\beta d_2 \cos(\Phi)] \\ \vdots \\ \exp[j(M-1)\beta d_M \cos(\Phi)] \end{bmatrix} \tag{8}$$

The symbol d denotes the distance between every two adjacent elements in terms of the wavelength (λ), and β represents the propagation phase constant:

$$\beta = \frac{2\pi}{\lambda} \tag{9}$$

In fact, the array factor is exactly equal to the antenna radiation pattern if the antenna elements are omnidirectional [37]. Figure 3b illustrates the general form of the array factor of an arbitrary antenna array. It is clear that the array factor consists of the main beam (major lobe) and minor lobes. The two minor lobes adjacent to the main beam are called the side lobes, and they are often with the highest level compared to the other minor lobes. To set the main beam toward $\Phi = 90^{\circ}$ the excitation phase angle between the excitation current of each antenna element should be equal to 0°. In other words, the weights vector ($\boldsymbol{w}$) has real values since the phase of this vector is set to zero in this work.

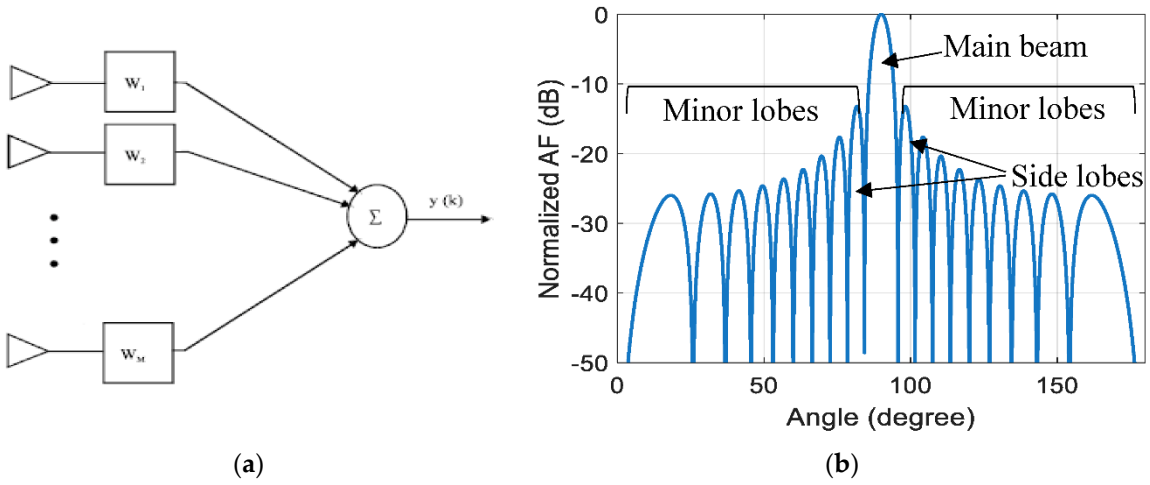

(**a**) (**b**)

Figure 3. Antenna array (**a**) structure and (**b**) the array factor in dB.

It should be noted that the optimization process is applied under the following conditions:

1. Array size is 20-element.
2. Fungi population size is 50.

3. $MT_{min} = 20$ and $MT_{max} = 60$.
4. Immobile expansion factor $IEF = 0.01$.
5. Number of hyphae $hyp = 10$.
6. Fungi dispersion = 5.
7. Number of runs = 30.

It is important to note that the immobile mass expansion requires to apply the fitness function on each hyphen, so the actual number of steps for the entire optimization is given by:

$$Actual\ number\ of\ steps = number\ of\ steps \times hyp \tag{10}$$

Consequently, to make a fair comparison with the other algorithms, the number of steps applied for the other algorithms will be (hyp) times the number of steps of the FKE algorithm.

The antenna array can be manipulated in two ways:

- Linear Optimization: by optimizing the magnitude of the weight vector.
- Nonlinear optimization: by optimization the inter-element spacing d.

4.1. Side Lobe Reduction

This section is about optimizing the sidelobe ratio (SLR) of the antenna array which is given by:

$$SLR_{dB} = 20\ log\left(\frac{mainbeam\ level}{side\ lobe\ level}\right) \tag{11}$$

It is well-known that decreasing the width of the main beam results in a very good concentration of electromagnetic energy toward the target, but it also results in a higher sidelobe level. It is found that the uniform distribution (equal excitation amplitudes and equal element spacing) provides the narrowest beam compared to the other distributions but with the highest side lobes [38]. The optimization problem in this subsection is concluded by: providing a beam width as narrow as that of the uniform distribution but with SLR as high as possible.

4.1.1. Side Lobe Reduction by Optimizing the Excitation Magnitude

This sub-section is about optimizing the SLR_{dB} to be larger than 22 dB under the constraint of narrow main beamwidth via optimizing the magnitude ($\boldsymbol{w}$) of the excitation current (as given in Equation (7)) of the antenna element while keeping the inter-element spacing equal to $d = 0.5\lambda$. As mentioned earlier, the width of the main beam (null-to-null beam width) is chosen to be equal to that of the uniform distribution which is equal to 14°. Therefore, the fitness function is based on the following condition:

$$Fitness = \begin{cases} \max(SLR_{\mathrm{dB}}) \\ with\ beamwidth\ equal\ to\ that\ of\ the\ uniform\ dstribution \end{cases} \tag{12}$$

Table 1 demonstrates a comparison between the success rate of the proposed FKE algorithm with that of some other well-known optimization algorithms. The success rate is given by:

$$SR\% = \frac{nunumber\ of\ successful\ runs}{total\ number\ of\ runs} \times 100\% \tag{13}$$

It is clear that the SR of the proposed algorithm is perfect for this kind of problem. Table 2 gives the best excitation magnitude that results in $SLR_{dB} = 25.6023$ dB with null-to-null beam width equal to 14°. Figure 4 illustrates a comparison between the normalized array factor (in dB) resulting from the FKE algorithm and that of the uniform distribution. The sidelobe reduction can clearly be seen from this figure for the same number of antenna elements.

Table 1. The success rate (SR) of the proposed FKE algorithm, PSO, and GA for the sidelobe reduction using the magnitude of the excitation current (No. of runs = 30).

Algorithm	Best SLR (dB)	SR %
FKE (30 iterations)	25.6023	100
PSO (300 iterations)	24.6177	73.33
GA (300 iterations)	24.8263	66.67

Table 2. The best normalized value of the magnitude of the excitation current of FKE.

Element No.	Excitation Magnitude
1	0.3963
2	0.3788
3	0.4980
4	0.4905
5	0.5334
6	0.7778
7	0.8593
8	0.8714
9	0.9791
10	0.9578
11	0.9376
12	1.0000
13	0.9482
14	0.7375
15	0.8107
16	0.6890
17	0.6734
18	0.3582
19	0.4529
20	0.4590

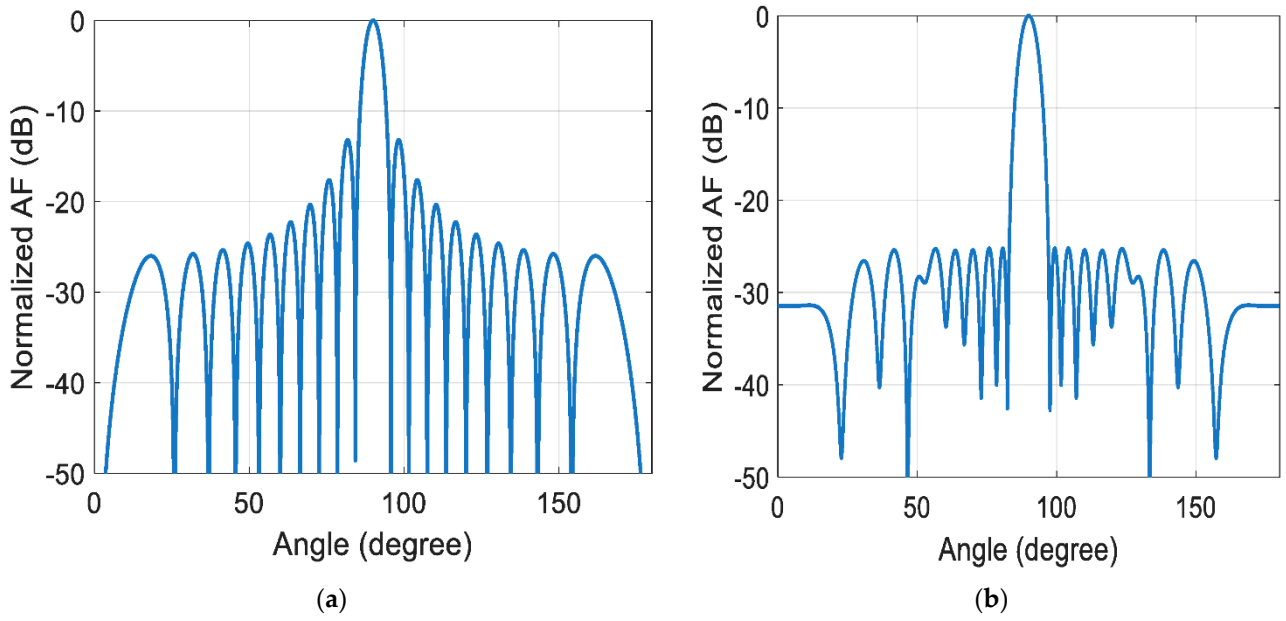

Figure 4. The normalized array factor for 2- element array antenna (**a**) using uniform distribution and (**b**) using FKE optimization.

4.1.2. Side Lobe Reduction by Optimizing the Enter Element Spacing

Based on Equation (7), the scenario of this optimization problem is concluded by exciting the antenna elements with an equal amount of current magnitude while optimizing the inter-element spacing (d with respect to λ) in order to obtain a large SLR with a narrow beam. The range of the element-spacing is chosen to be $[0 \rightarrow \lambda]$. The fitness function is exactly the same as that given in (12). The success rate of the FKE algorithm compared to some other prominent algorithms is given in Table 3, whereas the inter-element spacing corresponding to the best SLR is shown in Table 4. The success rate of the proposed algorithm for $SLR_{dB} \geq 22$ dB is also superior to that of the other algorithms in this type of problem. The normalized array factor corresponding to the best element spacing is shown in Figure 5 which also shows a noticeably reduced sidelobe level.

Table 3. The success rate (SR) of the proposed FKE algorithm, PSO, and GA for the sidelobe reduction using the inter-element spacing (No. of runs = 30).

Algorithm	Best SLR (dB)	SR %
FKE (30 iterations only)	24.0017	100
PSO (300 iterations)	22.5721	40
GA (300 iterations)	22.3245	33.33

Table 4. The best normalized value of inter-element spacing with respect to the wavelength (λ) using FKE.

Element No.	Normalized Element Spacing
1–2	0.8138
2–3	0.7410
3–4	0.5958
4–5	0.3971
5–6	0.4453
6–7	0.4016
7–8	0.3914
8–9	0.3398
9–10	0.4283
10–11	0.2739
11–12	0.3961
12–13	0.3602
13–14	0.3708
14–15	0.3773
15–16	0.4626
16–17	0.5098
17–18	0.4441
18–19	0.6857
19–20	0.7318

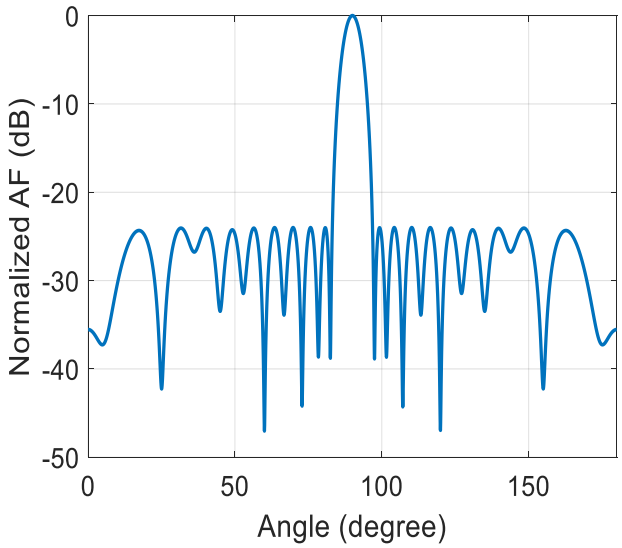

Figure 5. The normalized array factor for 20 element array antenna by optimizing the inter-element spacing of the array antenna using FKE algorithm.

4.2. Flat-Top Pattern

This sub-section is about obtaining a wide beam with a flat-top pattern to transmit an equal amount of radiation to the intended area with the constraint of a low sidelobe level. In fact, this optimization problem is too complicated, so it is required two steps of optimization. The first step includes providing a flat top regardless of the sidelobe level by optimizing the excitation magnitude only. Thence, the optimization of the sidelobe levels starts by modifying the inter-element spacing under the constraint of the obtained flat-top pattern.

4.2.1. Step 1: Flat-Top Pattern Regardless the SLR

This pattern is obtained by optimizing the magnitude of the excitation ($\boldsymbol{w}$) with $d = 0.5\lambda$. The constraint is to obtain a ripple value less than 0.5 dB within the required azimuth angle range. Therefore, the fitness function that describes this problem is given by:

$$Fitness = \begin{cases} \text{for } \Phi_{min} \leq \Phi \leq \Phi_{max} \\ |AF_{max} - AF(\Phi)| \leq 0.5 \text{ dB} \end{cases} \tag{14}$$

where AF_{max} represents the maximum value of the array factor in dB which is equal to 0 dB for the normalized array factor. In this work, the azimuth angle range is set to be as $\Phi_{min} = 80^{\circ}$ and $\Phi_{max} = 100^{\circ}$. Table 5 shows the success rate of the FKE algorithm compared to some other algorithms, and the proposed algorithm surpasses the others by its 100% success rate. The weights vector that is corresponding to the best solution that the algorithm provides is listed in Table 6. The resulted normalized array factor of the optimized antenna is exhibited in Figure 6. The flat-top pattern is clearly obvious from this figure within the intended azimuth angle range, while the side lobe is quite high.

Table 5. The success rate (SR) of the proposed FKE algorithm, PSO, and GA for the flat-top pattern. (No. of runs = 30).

Flat-Top Regardless SLR			Flat-Top with Reduced Side Lobes		
Algorithm	**Best Flat-Top Ripple (dB)**	**SR %**	**Algorithm**	**Best SLR (dB)**	**SR %**
FKE 50 iterations only	0.1044	100	FKE 30 iterations only	23.4612	100
PSO 500 iterations	0.2785	56.67	PSO 300 iterations	21.6342	43.33
GA 500 iterations	0.2255	46.67	GA 300 iterations	20.8564	30

Table 6. The best normalized value of the amplitude of the excitation current and element spacing with respect to λ using FKE for flat-top pattern.

Flat-Top Regardless SLR		Flat-Top with Reduced Side Lobes	
Element No.	**Excitation Amplitude**	**Element No.**	**Normalized Element Spacing**
1	−0.0126	1–2	0.3906
2	−0.3447	2–3	0.6579
3	−0.0309	3–4	0.6475
4	0.6800	4–5	0.4998
5	0.8999	5–6	0.2645
6	0.7992	6–7	0.3324
7	1.0000	7–8	0.3306
8	0.9985	8–9	0.4204
9	0.9001	9–10	0.4749
10	0.2385	10–11	0.4494
11	−0.1494	11–12	0.4343
12	−0.2813	12–13	0.2418
13	0.0128	13–14	0.2037
14	−0.3478	14–15	0.6407
15	−0.2256	15–16	0.3431
16	0.3540	16–17	0.5052
17	0.1807	17–18	0.1562
18	−0.1175	18–19	0.4494
19	0.3787	19–20	0.1466
20	−0.3687		

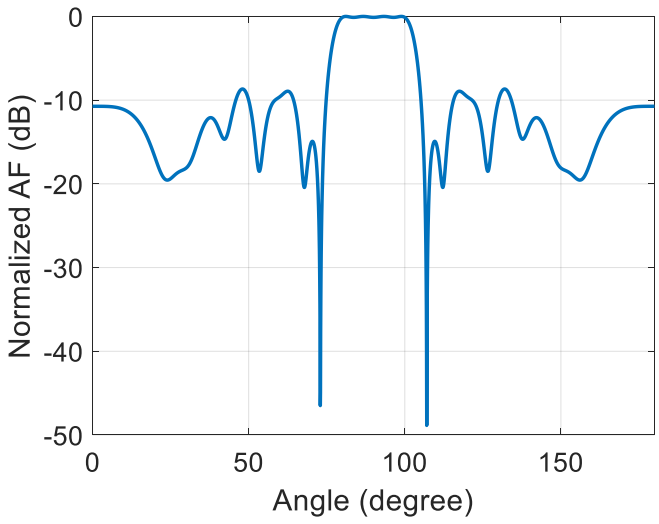

Figure 6. The normalized flat-top array factor for 20 element array antenna by modifying the excitation amplitude of the array antenna using FKE algorithm.

4.2.2. Step 2: Flat-Top Pattern with Reduced Side Lobes

After optimizing the flatness of the main beam, SLR larger than 20 dB is achieved by modifying the inter-element spacing while keeping the excitation magnitude as given in the previous step. The fitness function consists of two parts. The first part is exactly the same as the one given in (12) but with a beam width equal to 40°, whereas the second part is the same as the fitness condition of (14) to keep the flatness of the main beam. The success rate of the FKE algorithm is found to be 100%, and it is superior to the other algorithms as given in Table 5. On the other hand, Table 6 lists the inter-element spacing with respect to the wavelength that results in the best solution for the proposed antenna. The obtained normalized flat-top array factor with reduced side lobes is illustrated in Figure 7.

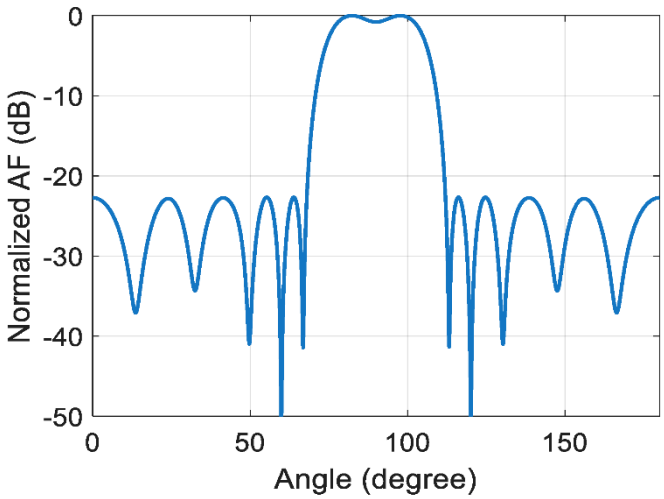

Figure 7. The normalized array factor for 20 element array antenna by modifying the inter-element spacing of the array antenna using FKE.

4.3. Triangular Beam Pattern

This section is about obtaining a wide beam with a triangular pattern to focus the transmitted power of the radiation toward the intended area with the constraint of low sidelobe level. Therefore, it also requires two steps.

4.3.1. Step 1: Triangular Beam Regardless the Side Lobe Level

The magnitude of the excitation of the antenna elements ($\boldsymbol{w}$) is optimized in this problem to obtain a triangular edge in the main beam of the radiation pattern (with $d = 0.5\lambda$). The problem is to provide a pattern with almost a straight line with a positive slope in the range $[85^{\circ} \rightarrow 90^{\circ}]$, and another straight line with a negative slope along with the range $[90^{\circ} \rightarrow 95]$. Luckily, since the excitation weights are real, the pattern of the array factor is symmetric. Therefore, the optimization process deals with the angular range $[90^{\circ} \rightarrow 95]$, and the symmetry of the pattern has the custody of generating the other straight line within the range $[85^{\circ} \rightarrow 90]$. As a result, the fitness function corresponding to generating the triangular shape pattern is given by:

$$Fitness = \begin{cases} for\ 90^{\circ} \leq \Phi \leq 95^{\circ} \\ \left\{ \left| AF(\Phi) - \left(-2\left(\Phi \times \frac{180}{\pi} - 90^{\circ} \right) \right) \right| \right\} \leq 1 \text{ dB} \end{cases} \quad (15)$$

The success rate of the FKE algorithm versus some other well-known algorithms is demonstrated in Table 7, and the weights vector that results in the best triangular shape is given in Table 8. In this problem, FKE algorithm results in a perfect success rate equal to 100%. Figure 8 illustrates the normalized array factor with a triangular shape regardless of the value of the sidelobe level.

Table 7. The success rate (SR) of the proposed FKE algorithm, PSO, and GA for the triangular pattern. (No. of runs = 30).

Triangular Pattern Regardless SLR			Triangular Pattern with Reduced Side Lobes		
Algorithm	**Best Triangular Pattern Ripple (dB)**	**SR %**	**Algorithm**	**Best SLR (dB)**	**SR %**
FKE (50 iterations only)	0.6345	100	FKE 30 iterations only	19.0123	100
PSO (500 iterations)	0.7353	96.67	PSO 300 iterations	20.2093	30
GA (500 iterations)	0.6453	93.33	GA 300 iterations	19.5364	36.67

Table 8. The best normalized value of the amplitude of the excitation current and element spacing with respect to λ using FKE for triangular pattern.

Triangular Pattern Regardless SLR		Triangular Pattern with Reduced Side Lobes	
Element No.	**Excitation Amplitude**	**Element No.**	**Normalized Element Spacing**
1	0.8004	1–2	0.3906
2	0.2412	2–3	0.6579
3	−0.2876	3–4	0.6475
4	−0.2911	4–5	0.4998
5	0.1939	5–6	0.2645
6	0.0115	6–7	0.3324
7	−0.0081	7–8	0.3306
8	0.3175	8–9	0.4204
9	0.4632	9–10	0.4749
10	0.6449	10–11	0.4494
11	0.9564	11–12	0.4343
12	1.0000	12–13	0.2418
13	0.6030	13–14	0.2037
14	0.8111	14–15	0.6407
15	0.4692	15–16	0.3431
16	−0.1326	16–17	0.5052
17	−0.0892	17–18	0.1562
18	0.3432	18–19	0.4494
19	0.3022	19–20	0.1466
20	0.3836		

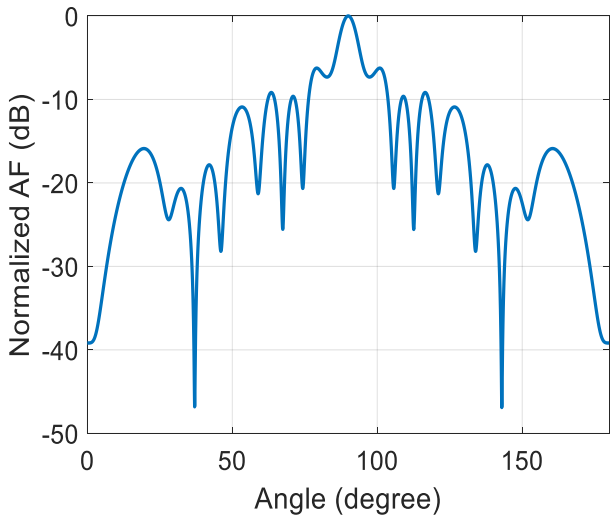

Figure 8. The normalized triangular-shaped array factor for 20 element array antenna by modifying the excitation amplitude of the array antenna using FKE.

4.3.2. Step 2: Triangular Pattern with Reduced Side Lobes

The side lobe of the triangular pattern can also be reduced by optimizing the inter-element spacing between the antenna elements while keeping the excitation magnitude as that given in Table 8. The fitness function of this problem is also with two parts. The first part ensures the reduction of the sidelobe using (12), while the second part is a condition that maintains the triangular shape of the main beam as given in (14). The success rate (for SLR < 18 dB) of the FKE algorithm given in Table 7 is found to be 100%, and it clearly surpasses the other algorithms. On the other hand, the list of the inter-element spacing with respect to the wavelength that results in the best solution for the proposed antenna is demonstrated in Table 8. The obtained normalized triangular-shaped array factor with reduced side lobes is exhibited in Figure 9.

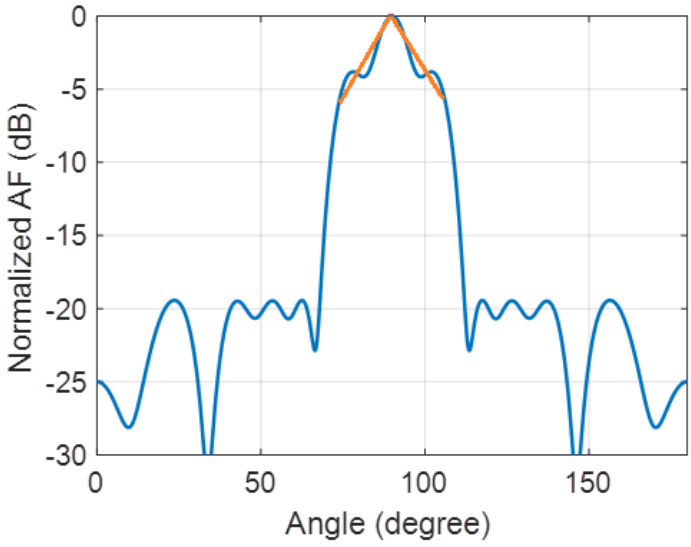

Figure 9. The normalized triangular array factor for 20 element array antenna by modifying the inter-element spacing of the array antenna using FKE algorithm.

4.4. Anti-Jamming System

Anti-jamming smart antennas are substantial in military applications especially in those vulnerable to intentional jamming that may be transmitted by the enemies. Figure 10 reveals the parameters of M-element anti-jamming antenna system with its operation concept. The desired transmitted signal is in line of sight (LOS) with the antenna array of this system. The jamming signals are transmitted from different directions to interfere with the desired signal or to send fake information to the receiver. As shown in Figure 10, the anti-jamming antenna system should adjust its main beam in the direction of the desired signal and orient radiation nulls toward the directions of the jamming signals. The conventional beam-forming algorithms can orient its main beam toward the desired direction, but unfortunately, they can only attenuate the jamming signals especially with highly correlated jamming signals [37]. Since the jamming signals sometimes have power values higher than that of the desired signal itself, the attenuation is inefficient in these kinds of problems. In fact, FKE algorithm is independent of the correlation between signals, so it can perfectly reject the jamming signals by positioning radiation nulls toward them regardless of their amount of transmitted power. The output signal (y) of the anti-jamming antenna array is given by [37]:

$$y = \boldsymbol{w}^{\boldsymbol{H}}\, \boldsymbol{x} \tag{16}$$

where

$$\boldsymbol{x} = \sum_{k=0}^{K} \sqrt{P_k}\, \boldsymbol{a_k} \tag{17}$$

where K represents the number of the received signals, P_k the power value of each signal, and $\boldsymbol{a_k}$ is the steering vector of each signal which is given by:

$$\boldsymbol{a_k} = \begin{bmatrix} 1 \\ \exp[j\beta d\cos(\Phi_k)] \\ \exp[j2\beta d\cos(\Phi_k)] \\ \vdots \\ \exp[j(M-1)\beta d\cos(\Phi_k)] \end{bmatrix} \quad (18)$$

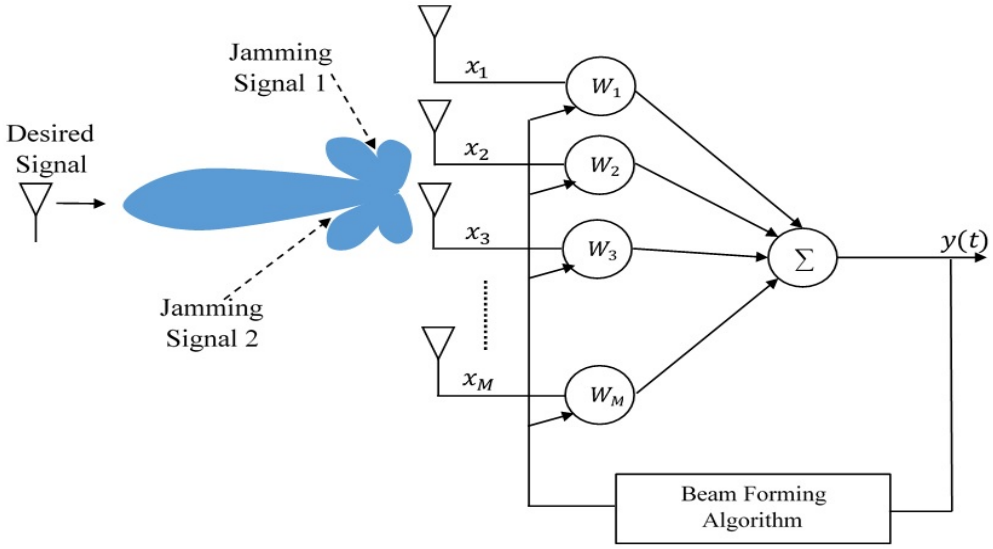

Figure 10. Smart antenna system with M-antenna elements [39].

The problem that is wanted to be solved in this work is that there is a desired signal with signal power equal to $P_o watt$ at $\Phi_o = 90^\circ$ with the presence of eight interfering signals. The power values of the eight jamming signals are as follows: $[3P_o, 2P_o, 3P_o, 2P_o, 3P_o, 2P_o, 3P_o, 2P_o]$, and their angle of arrivals are as follows: $[20^\circ, 40^\circ, 50^\circ, 55^\circ, 110^\circ, 120^\circ, 130^\circ, 145^\circ]$, respectively. The magnitude of the excitation vector ($\boldsymbol{w}$) is the parameter to be optimized with $d = 0.5\lambda$. The fitness function that is suitable for this kind of problem is given by:

$$Fitness = \min\left[\left|\sqrt{P_o} - \left|\boldsymbol{w}^H \boldsymbol{x}\right|\right|\right] \quad (19)$$

Table 9 reveals the perfect success rate of FKE and all the other algorithms in solving this problem, and the optimum magnitude of excitation is given in Table 10. The resulted antenna-normalized array factor is shown in Figure 11 at which the main beam is forwarded toward the desired signal and all the jamming signals are eliminated by locating radiation nulls in their directions.

Table 9. The success rate (SR) of the proposed FKE algorithm, PSO, and GA for the anti-jamming smart antenna system (No. of runs = 30).

Algorithm	SR %
FKE (30 iterations only)	100
PSO (300 iterations)	100
GA (300 iterations)	100

Table 10. The best normalized value of the magnitude of the excitation current using FKE algorithm for anti-jamming optimization.

Element No.	Excitation Amplitude
1	0.2876
2	0.5281
3	0.7154
4	1.0000
5	0.6386
6	0.7782
7	0.5270
8	0.5188
9	0.5191
10	0.3633
11	0.3661
12	0.3836
13	0.4718
14	0.4543
15	0.7104
16	0.7682
17	0.9019
18	0.9885
19	0.4997
20	0.4370

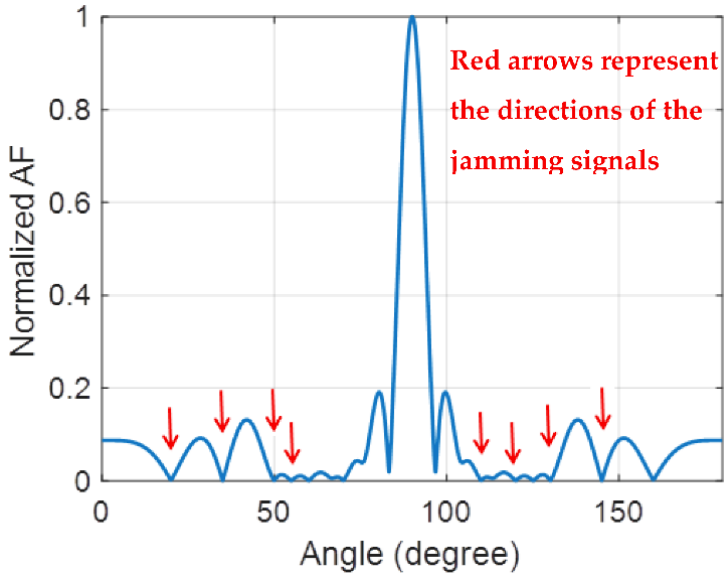

Figure 11. The normalized array factor for 20-element anti-jamming antenna by optimizing the excitation amplitude of the array antenna using FKE algorithm.

5. Results Discussion

This section includes a comparison between the performance of the FKE algorithm and those of the PSO and GA in terms of the average CPU time, memory size, and success rate. Actually, the CPU time and the memory size were calculated for all problems discussed in the previous section, and then the resulted numbers were averaged to give a concise and clear comparison scenario. The algorithms were executed using a computer with the following specifications: Processor (Intel (R) Core(TM) i7), RAM 16 GB. Table 11 lists the CPU time average, the average memory size, and the average success rate of the FKE algorithm, PSO, and GA. As mentioned in Section 4, the immobile mass results in extending the number of hyphae, and this makes the total number of iteration of the FKE multiplied by the number of hyphae as given in Equation (10). For this reason, the memory size of

FKE is larger than that of the PSO and GA. However, the average CPU time is almost the same for the three algorithms because the number of steps of the FKE algorithm should be equal to that of the PSO and GA divided by the number of hyphae (as discussed in Section 4). Nevertheless, the precision of the proposed FKE algorithm is highlighted by its perfect average success rate in solving the aforementioned antenna array problems where the average SR of the proposed algorithm is equal to 100%.

Table 11. The average CPU time, average memory size, and the average SR of FKE algorithm compared to that of the PSO and GA.

Algorithm	Average CPU Time (s)	Average Memory Size (byte)	Average SR %
FKE (30 iterations)	30.863	4,046,848	100
PSO (300 iterations)	31.387	2,072,576	62.857
GA (300 iterations)	28.614	1,975,724	58.906

Generally, antenna array problems are single-objective problems. Therefore, as a future work, the effectiveness of the FKE algorithm will be studied for multi-objective optimizations problems since this require completely different applications and different sets of results.

6. Conclusions

A new optimization algorithm based on the Fungi Kingdom Expansion (FKE) behavior has successfully been implemented for antenna array beamforming problems. The chaotic immobile mass expansion, deterministic mobile mass expansion, and the random dispersion of the fungi are utilized for optimizing the magnitude of the excitation and/or the inter-element spacing to attain the required shape of the antenna array factor. The algorithm is applied on a 20-element antenna array to solve the problem of the side lobe reduction, flat-top pattern, triangular pattern, and anti-jamming system. The performance of the proposed algorithm is statistically compared with some other prominent optimization algorithms, and the proposed antenna gives a 100% success rate for all of the aforementioned problems.

Author Contributions: Conceptualization, F.M.A., D.S. and Y.I.A.A.-Y.; methodology, F.M.A.; investigation, F.M.A., Y.I.A.A.-Y., D.S., R.S.A., C.H.S. and R.A.A.-A.; resources, F.M.A., D.S. and Y.I.A.A.-Y.; writing—original draft preparation, F.M.A., Y.I.A.A.-Y., D.S. and R.S.A.; writing—review and editing, F.M.A., Y.I.A.A.-Y., D.S., R.S.A., C.H.S. and R.A.A.-A.; visualization, F.M.A., Y.I.A.A.-Y., D.S., R.S.A., C.H.S. and R.A.A.-A. All authors have read and agreed to the published version of the manuscript.

Funding: This research received no external funding.

Conflicts of Interest: The authors declare no conflict of interest.

References

1. Mirjalili, S.; Lewis, A. The Whale Optimization Algorithm. *Adv. Eng. Softw.* **2016**, *95*, 51–67. [CrossRef]
2. Abualigah, L.; Diabat, A.; Mirjalili, S.; Abd Elaziz, M.; Gandomi, A.H. The Arithmetic Optimization Algorithm. *Comput. Methods Appl. Mech. Eng.* **2021**, *376*, 113609. [CrossRef]
3. Sattar, D.; Salim, R. A smart metaheuristic algorithm for solving engineering problems. *Eng. Comput.* **2021**, *37*, 2389–2417. [CrossRef]
4. Holland, J.H. *Adaptation in Natural and Artificial Systems: An Introductory Analysis with Applications to Biology, Control, and Artificial Intelligence*; MIT Press: Cambridge, MA, USA, 1992.
5. Mirjalili, S.; Mirjalili, S.M.; Lewis, A. Grey Wolf Optimizer. *Adv. Eng. Softw.* **2014**, *69*, 46–61. [CrossRef]
6. Ali, R.S.; Alnahwi, F.M.; Abdullah, A.S.J.A.J.o.E.; Engineering, E. A modified camel travelling behaviour algorithm for engineering applications. *Aust. J. Electr. Electron. Eng.* **2019**, *16*, 176–186. [CrossRef]

7. Naruei, I.; Keynia, F. Wild horse optimizer: A new meta-heuristic algorithm for solving engineering optimization problems. *Eng. Comput.* **2021**. [CrossRef]
8. Mirjalili, S.; Gandomi, A.H.; Mirjalili, S.Z.; Saremi, S.; Faris, H.; Mirjalili, S.M. Salp Swarm Algorithm: A bio-inspired optimizer for engineering design problems. *Adv. Eng. Softw.* **2017**, *114*, 163–191. [CrossRef]
9. Dorigo, M.; Birattari, M.; Stutzle, T.J.I.C.I.M. Ant colony optimization. *IEEE Comput. Intell. Mag.* **2006**, *1*, 28–39. [CrossRef]
10. Lalbakhsh, P.; Zaeri, B.; Lalbakhsh, A. An Improved Model of Ant Colony Optimization Using a Novel Pheromone Update Strategy. *IEICE Trans. Inf. Syst.* **2013**, *96*, 2309–2318. [CrossRef]
11. Wang, G.-G.J.M.C. Moth search algorithm: A bio-inspired metaheuristic algorithm for global optimization problems. *Memetic Comput.* **2018**, *10*, 151–164. [CrossRef]
12. Kennedy, J.; Eberhart, R. Particle swarm optimization. In Proceedings of the ICNN'95-International Conference on Neural Networks, Perth, Australia, 27 November–1 December 1995; pp. 1942–1948.
13. Lalbakhsh, A.; Afzal, M.U.; Esselle, K.P.; Smith, S. Design of an artificial magnetic conductor surface using an evolutionary algorithm. In Proceedings of the 2017 International Conference on Electromagnetics in Advanced Applications (ICEAA), Verona, Italy, 11–15 September 2017; pp. 885–887.
14. Lalbakhsh, A.; Esselle, K.P. Directivity improvement of a Fabry-Perot cavity antenna by enhancing near field characteristic. In Proceedings of the 2016 17th International Symposium on Antenna Technology and Applied Electromagnetics (ANTEM), Montreal, QC, Canada, 10–13 July 2016; pp. 1–2.
15. Yang, X.S.; Hossein Gandomi, A. Bat algorithm: A novel approach for global engineering optimization. *Eng. Comput.* **2012**, *29*, 464–483. [CrossRef]
16. Abdollahzadeh, B.; Gharehchopogh, F.S.; Mirjalili, S. African vultures optimization algorithm: A new nature-inspired metaheuristic algorithm for global optimization problems. *Comput. Ind. Eng.* **2021**, *158*, 107408. [CrossRef]
17. Akyol, S.; Alatas, B. Plant intelligence based metaheuristic optimization algorithms. *Artif. Intell. Rev.* **2017**, *47*, 417–462. [CrossRef]
18. Li, M.D.; Zhao, H.; Weng, X.W.; Han, T. A novel nature-inspired algorithm for optimization: Virus colony search. *Adv. Eng. Softw.* **2016**, *92*, 65–88. [CrossRef]
19. Al-Betar, M.A.; Alyasseri, Z.A.A.; Awadallah, M.A.; Abu Doush, I. Coronavirus herd immunity optimizer (CHIO). *Neural Comput. Appl.* **2021**, *33*, 5011–5042. [CrossRef] [PubMed]
20. Hatamlou, A. Heart: A novel optimization algorithm for cluster analysis. *Prog. Artif. Intell.* **2014**, *2*, 167–173. [CrossRef]
21. Jaddi, N.S.; Alvankarian, J.; Abdullah, S. Kidney-inspired algorithm for optimization problems. *Commun. Nonlinear Sci. Numer. Simul.* **2017**, *42*, 358–369. [CrossRef]
22. Hashim, F.A.; Hussain, K.; Houssein, E.H.; Mabrouk, M.S.; Al-Atabany, W. Archimedes optimization algorithm: A new metaheuristic algorithm for solving optimization problems. *Appl. Intell.* **2021**, *51*, 1531–1551. [CrossRef]
23. Azizi, M. Atomic orbital search: A novel metaheuristic algorithm. *Appl. Math. Model.* **2021**, *93*, 657–683. [CrossRef]
24. Alatas, B. ACROA: Artificial Chemical Reaction Optimization Algorithm for global optimization. *Expert Syst. Appl.* **2011**, *38*, 13170–13180. [CrossRef]
25. Abdechiri, M.; Meybodi, M.R.; Bahrami, H. Gases Brownian Motion Optimization: An Algorithm for Optimization (GBMO). *Appl. Soft Comput.* **2013**, *13*, 2932–2946. [CrossRef]
26. Mirjalili, S. SCA: A sine cosine algorithm for solving optimization problems. *Knowl. Based Syst.* **2016**, *96*, 120–133. [CrossRef]
27. Das, B.; Mukherjee, V.; Das, D. Student psychology based optimization algorithm: A new population based optimization algorithm for solving optimization problems. *Adv. Eng. Softw.* **2020**, *146*, 102804. [CrossRef]
28. Geem, Z.W.; Kim, J.H.; Loganathan, G.V.J.S. A new heuristic optimization algorithm: Harmony search. *Simulation* **2001**, *76*, 60–68. [CrossRef]
29. Fadakar, E.; Ebrahimi, M. A new metaheuristic football game inspired algorithm. In Proceedings of the 2016 1st Conference on Swarm Intelligence and Evolutionary Computation (CSIEC), Bam, Iran, 9–11 March 2016; pp. 6–11.
30. Kaveh, A.; Khanzadi, M.; Rastegar Moghaddam, M. Billiards-inspired optimization algorithm; a new meta-heuristic method. *Structures* **2020**, *27*, 1722–1739. [CrossRef]
31. Lalbakhsh, A.; Afzal, M.U.; Hayat, T.; Esselle, K.P.; Mandal, K. All-metal wideband metasurface for near-field transformation of medium-to-high gain electromagnetic sources. *Sci. Rep.* **2021**, *11*, 9421. [CrossRef]
32. Lalbakhsh, A.; Afzal, M.U.; Esselle, K.P.; Smith, S.L. Low-Cost Nonuniform Metallic Lattice for Rectifying Aperture Near-Field of Electromagnetic Bandgap Resonator Antennas. *IEEE Trans. Antennas Propag.* **2020**, *68*, 3328–3335. [CrossRef]
33. Afzal, M.U.; Esselle, K.P.; Lalbakhsh, A. A Methodology to Design a Low-Profile Composite-Dielectric Phase-Correcting Structure. *IEEE Antennas Wirel. Propag. Lett.* **2018**, *17*, 1223–1227. [CrossRef]
34. Hayat, T.; Afzal, M.U.; Lalbakhsh, A.; Esselle, K.P. Additively Manufactured Perforated Superstrate to Improve Directive Radiation Characteristics of Electromagnetic Source. *IEEE Access* **2019**, *7*, 153445–153452. [CrossRef]
35. Bento, C.R.d.C.; Wille, E.C.G. Bio-inspired routing algorithm for MANETs based on fungi networks. *Ad Hoc Networks* **2020**, *107*, 102248. [CrossRef]
36. Wolpert, D.H.; Macready, W.G. No free lunch theorems for optimization. *IEEE Trans. Evol. Comput.* **1997**, *1*, 67–82. [CrossRef]
37. Godara, L.C. *Smart Antennas*; CRC press: Boca Raton, FL, USA, 2004.
38. Balanis, C.A. *Antenna Theory and Design*; John Wiley & Sons: Hoboken, NJ, USA, 2016.
39. Singh, J.; Pal, A. A Smart Antenna Beamforming Using LMS Adaptive Filter Algorithm. *Semant. Scholar.* **2014**, *1*, 1–3. [CrossRef]